Colloids and Surfaces A: Physicochem. Eng. Aspects 384 (2011) 668–674

Contents lists available at ScienceDirect

Colloids and Surfaces A: Physicochemical and Engineering Aspects

journal homepage: www.elsevier.com/locate/colsurfa

LSPR and SAXS studies of starch stabilized Ag–Cu alloy nanoparticles

Manjeet Singh [a], I. Sinha [a,*], A.K. Singh [c], R.K. Mandal [b]

[a] Department of Applied Chemistry, Institute of Technology, Banaras Hindu University, Varanasi 221005, India
[b] Department of Metallurgical Engineering, Centre of Advanced Study, Institute of Technology, Banaras Hindu University and Unit of Nanoscience and Technology, BHU, Varanasi 221005, India
[c] Defence Metallurgical Research Laboratory, Kanchanbagh P.O., Hyderabad 500058, India

ARTICLE INFO

Article history:
Received 9 February 2011
Received in revised form 20 April 2011
Accepted 19 May 2011
Available online 27 May 2011

Keywords:
Ag–Cu alloy nanoparticles
SAXS analysis
Fractal aggregates
Localized surface plasmon resonance

ABSTRACT

We report the aqueous phase chemical reduction synthesis of starch stabilized Ag–Cu alloy nanoparticles. Changing the proportions of Ag and Cu precursor salts leads to different levels of solid solubility. The variations in the localized surface plasmon resonance (LSPR) absorbance of sols are analyzed from the perspective of nanoparticles composition and their structural features. Small angle X-ray scattering (SAXS) analysis of the Ag–Cu nanoparticles sols shows the formation of mass fractal aggregate nanostructures in all cases.

1. Introduction

The nature of absorption due to localized surface plasmon resonance (LSPR) in noble metal nanoparticle sols depends on the nanoparticle material, size, shape, and aspect ratio [1,2]. For alloys, LSPR is sensitive to compositions and their variations. In addition to these, LSPR behavior is also sensitive to the dielectric properties of the surrounding medium and the inter-particle separation [3,4]. In case two nanoparticles approach each other to within distances less than their size, interaction between their sphere of influence leads to inter-particle plasmon coupling, broadening and red-shifting the LSPR absorbance peaks [3]. Sensor applications are either based on such aggregation induced LSPR changes or LSPR shifts due to changes in the local refractive index of the medium [5–7]. However, making the composition of nanoparticle a variable can bring out significant changes in the LSPR spectrum. Such an effect can be realized by synthesis of alloy nanoparticles [8].

In this context, an important issue pertains to the possibility of enhancing solid solubility of components in such small finite systems (nanoparticles) [9,10] at room temperature. The Ag–Cu alloy system, with an equilibrium phase diagram showing simple eutectic behavior with a wide range of miscibility gap at ambient temperature seems to be particularly suitable for such studies. Besides interesting LSPR behavior, Ag–Cu ultrafine or nanoparticles have a range of other prospective applications. These pertain to improved lead-free interconnect, dental amalgams, etc. [11,12]. Ag–Cu alloy NP could also provide interesting opportunities in the fast developing field of antibacterial materials. Materials capable of slow Ag(I) release, like Ag NP [13], and Cu(II) salts [14,15] are efficient antibacterial agents. Latest research has demonstrated that materials capable of Cu(II) and Ag(I) simultaneous release from surface have an enhanced antibacterial action [16].

We note that the size difference between Ag and Cu is less than 15% and both have face centered cubic (fcc) structure. Therefore, according to the Hume–Rothery rules Ag and Cu should form solid solution. The observation of enhanced solid solubilities under metastable condition conforms to this. Liquid phase chemical reduction routes are integral to the synthesis of such alloy nanoparticle sols. The choice of precursors, reducing and stabilizing agents is critical to the nature of alloy NPs sols desired. Moreover, changes in dispersant media such as pH and ionic strength can cause nanoparticle destabilization and aggregation. A few attempts have been made to prepare [12,17] Ag–Cu alloy NPs by chemical reduction techniques, especially from the perspective of studying their LSPR characteristics in sols. Hongjin et al. [12] have reported the synthesis and the LSPR behavior of phase-separated Ag–Cu nanoparticles sols. In their investigation, copper acetate hydrate and silver nitrate were added sequentially for preparation of Ag–Cu nanoparticles with poly(vinylpyrrolidone) (PVP) as a stabilizer in ethylene glycol. In a recent study, Cu shell on Ag-rich core and Ag shell on Cu-rich core bimetallic nanoparticles have been synthesized by the conventional polyol route [18]. We had earlier shown that Ag–Cu ultra-fine particles with varied degrees of solid solubility could also be prepared in an aqueous medium [19]. Hydrazine

* Corresponding author. Tel.: +91 542 2454072.
E-mail address: isinha.apc@itbhu.ac.in (I. Sinha).

0927-7757/$ – see front matter © 2011 Elsevier B.V. All rights reserved.
doi:10.1016/j.colsurfa.2011.05.037

hydrate was used to effect the aqueous co-reduction of silver nitrate and copper nitrate. The preparation was carried out in presence of PVP as stabilizer. The maximum solid solubilities of Cu in Ag and Ag in Cu were found to be ~18 at.% and ~3 at.%, respectively. However, alloy particles formed were >100 nm. Thus, the LSPR of the stable sol displayed only the characteristic silver nanoparticle absorbance.

In the present study we report the synthesis of Ag–Cu NPs by chemical reduction route in aqueous medium. Our object is to investigate this complex interplay between LSPR changes due to nanoparticle aggregation and that due to alloy formation. The synthesis is in situ and starch is used to stabilize the dispersions. Recent investigations have shown that in comparison to the stabilizing effect of PVP and PVA, starch as a dispersing agent is more effective in restricting the size of nanostructures formed [20]. We use SAXS to study the nano aggregates formed in the sol state and try to understand LSPR absorbance changes from this perspective. It is important to appreciate that in view of the length scale of the nanoparticle aggregate structures, which affects or induces LSPR changes, small angle X-ray scattering (SAXS) is the most appropriate non-invasive technique for such investigations. In conventional analysis by invasive microscopic techniques such as SEM and TEM, the substrate–particle interactions and the solvent drying kinetics may affect the nanostructures formed. Such techniques, therefore, may not be helpful for analyzing sol structures and thereby correlating the same with LSPR behavior.

2. Experimental

$AgNO_3$ and $Cu(NO_3)_2{\cdot}3H_2O$ were taken in a definite ratio and their aqueous solution prepared in 20 mL millipore water. One-gram starch was added and stirred until clear solution was obtained. Hydrazine hydrate (1 mL, 99–100%) and NaOH (1 mL, 1 M) were added in this solution under rapid stirring. A black precipitate was obtained immediately. Stirring was continued for the next 15-min to ensure completion of reaction. Different samples were made by changing the molar ratios of $AgNO_3$ and $Cu(NO_3)_2{\cdot}3H_2O$. The precipitate was washed with millipore water after filtration. The precipitate was then dried and the powder thus obtained was used for X-ray diffraction analysis. The filtrates thus obtained were starch stabilized stable sols of the Ag–Cu nanoparticles. A small volume of sol samples was now further diluted by a fixed factor to minimize inter-particle Van-der-waal interactions. This diluted sol was used for transmission electron microscope (TEM, Tecnai G^2, 200 keV) imaging, SAXS analysis and UV–visible spectroscopy (Cary Bio100 UV-vis Spectrophotometer). Samples for transmission electron microscope imaging were prepared by introducing a drop of this diluted sol on the carbon-coated copper grids and allowed to dry in a desiccator. SAXS data was collected using Panalytical X-ray generator (PW 3830) having SAXS 896986 Anton Paar mounted on it. The diluted sol was taken in the capillary sample holder (2 mL capacity) and placed in the X-ray apparatus for SAXS measurement. We recorded the SAXS data in the range of scattering vector (q) range of 0.053–6.5 nm^{-1}. The scattering intensity (Iq) versus q plots of the sols was obtained after subtracting the background scattering pattern of aqueous solution of starch.

All experiments, the UV–visible spectra and the XRD were repeated and found to be reproducible.

3. Results and discussion

3.1. XRD analysis of the starch stabilized Ag–Cu alloy NPs

The X-ray diffraction (XRD) of all samples were done at a scan speed of 0.25°/min. Extensive overlapping of Ag, Cu (of different levels of solid solubility) peaks, broadening and splitting of peaks

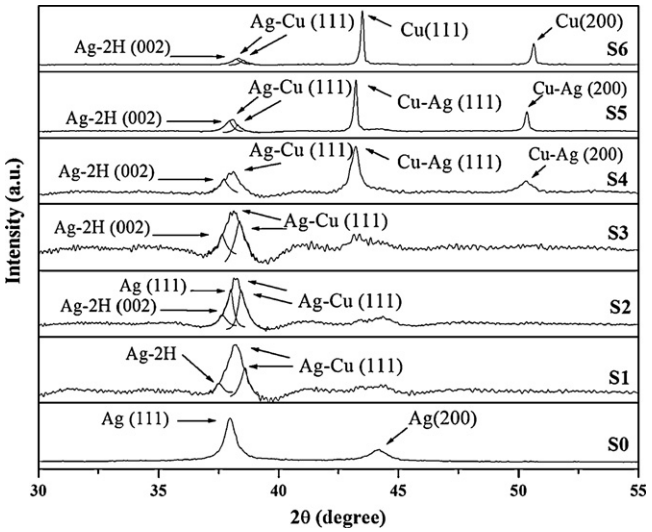

Fig. 1. XRD patterns of starch stabilized Ag–Cu alloy nanoparticles.

is observed. The major overlapping peaks are deconvoluted using standard routines to determine the peak positions and line widths. The lattice parameters of the identified phases are compared with the experimental data of Linde [21]. Alloying results in change of the lattice parameter from that of the pure element to one intermediate. The lattice parameter of the Ag–Cu alloys is found to be second order polynomial function of the solid solubility [21]. In the present work, all alloys compositions (in atomic percent, at.%) corresponding to experimentally determined lattice parameters have been found using this polynomial regression fit. Coherently scattered domain sizes are calculated by full width at half maximum (FWHM) using Scherrer formula after making necessary corrections for instrumental broadening. Hereafter, the solid solution phases that are Ag-rich are denoted by (Ag) and Cu-rich by (Cu).

The XRD patterns for various samples are shown in Fig. 1. Table 1 summarizes the quantitative details of the XRD analysis. Please note the lattice parameters for elemental Ag and Cu are 4.089 Å and 3.615 Å [21], respectively. As expected, sample S0 shows formation of FCC silver with the lattice parameter (4.09 Å) for the elemental Ag [21]. In the other samples, besides the FCC phase, the hexagonal 2H-(Ag) phase is also formed. Only the (0 0 2) line of the 2H-(Ag) phase is observed. The ICDD d-value for this plane is 2.395 Å. Similar values are reported for samples S1, S2 and S3. However, S4 onwards, the (0 0 2) line 2H-(Ag) phase d-value demonstrates progressive decrease with increase in $Cu(NO_3)_2{\cdot}3H_2O$ proportion in the initial composition. This may be due to increasing alloying of the 2H-(Ag) phase.

In S1, two FCC (Ag) (1 1 1) phases are formed with slightly different degrees of alloying. Similarly, in sample S2, pure FCC Ag phase and other FCC (Ag) phases with increasing solubility of Cu phases are found. For samples S3, S4 and S5, although there is some solid solubility of Cu in FCC (Ag), no coherent increase in solubility with initial $Cu(NO_3)_2{\cdot}3H_2O$ proportion is observed. The maximum solubility of (about ~10 at.%) Cu in (Ag) is obtained in S6. In addition, peak corresponding to the pure FCC Cu is also observed.

The domain size of all phases, in the samples considered, is in the nanometer range (Table 1). The domain size in case of nearly pure Ag phase is in the range of 11–13 nm. In contrast to this, the domain size for the phases showing appreciable alloying (>4 at.% Cu) seems to increase with the Cu at% in the FCC alloy phase. In fact, Fig. 2 shows that the domain size versus the alloy composition graph fits a second order polynomial function. Smaller domain size represents higher nucleation rate or slower growth rates. Therefore, increase